Brain Research 1646 (2016) 53–61

Contents lists available at ScienceDirect

Brain Research

journal homepage: www.elsevier.com/locate/brainres

Research report

Spatiotemporal changes in blood-brain barrier permeability, cerebral blood flow, T_2 and diffusion following mild traumatic brain injury

Wei Li [a,b], Lora Watts [a,c,d], Justin Long [a], Wei Zhou [a], Qiang Shen [a], Zhao Jiang [a], Yunxia Li [a], Timothy Q. Duong [a,b,*]

[a] Research Imaging Institute, University of Texas Health Science Center at San Antonio, TX 78229, USA
[b] Department of Ophthalmology, University of Texas Health Science Center at San Antonio, TX 78229, USA
[c] Department of Cellular and Structural Biology, University of Texas Health Science Center at San Antonio, TX 78229, USA
[d] Department of Neurology, University of Texas Health Science Center at San Antonio, TX 78229, USA

ARTICLE INFO

Article history:
Received 17 March 2016
Received in revised form
12 May 2016
Accepted 18 May 2016
Available online 18 May 2016

Keywords:
Traumatic brain injury
BBB permeability
Edema
Diffusion MRI
Dynamic contrast enhanced MRI

ABSTRACT

The blood-brain barrier (BBB) can be impaired following traumatic brain injury (TBI), however the spatiotemporal dynamics of BBB leakage remain incompletely understood. In this study, we evaluated the spatiotemporal evolution of BBB permeability using dynamic contrast-enhanced MRI and measured the volume transfer coefficient (K^{trans}), a quantitative measure of contrast agent leakage across the blood and extravascular compartment. Measurements were made in a controlled cortical impact (CCI) model of mild TBI in rats from 1 h to 7 days following TBI. The results were compared with cerebral blood flow, T_2 and diffusion MRI from the same animal. Spatially, K^{trans} changes were localized to superficial cortical layers within a 1 mm thickness, which was dramatically different from the changes in cerebral blood flow, T_2 and diffusion, which were localized to not only the superficial layers but also to brain regions up to 2.2 mm from the cortical surface. Temporally, K^{trans} changes peaked at day 3, similar to CBF and ADC changes, but differed from T_2 and FA, whose changes peaked on day 2. The pattern of superficial cortical layer localization of K^{trans} was consistent with patterns revealed by Evans Blue extravasation. Collectively, these results suggest that BBB disruption, edema formation, blood flow disturbance and diffusion changes are related to different components of the mechanical impact, and may play different roles in determining injury progression and tissue fate processes following TBI.

1. Introduction

The blood-brain barrier (BBB), which provides a stable biochemical environment for normal neuronal function, can be disrupted by the translational and rotational forces following traumatic brain injury (TBI). The loss of BBB integrity can lead to an imbalance of brain homeostasis including cerebral edema, inflammation, amongst others, which could result in pathophysiology including ischemia or neurodegeneration (Chodobski et al., 2011). The BBB has also been suggested as a target for therapeutic invention, as a normally functioning BBB is important for restoring brain hemostasis, and provides an optimal environment for neuronal repair (Shlosberg et al., 2010). While BBB damage is likely to occur in moderate to severe TBI, BBB damage in mild TBI and its relation to anatomical and physiological changes are less well understood. Evans Blue extravasation has been used to measure BBB leakage following TBI (Adelson et al., 1998; Başkaya et al., 1997; Dempsey et al., 2000), however, this method requires the sacrifice of the animals and does not permit longitudinal assessments to be made.

Dynamic contrast enhanced (DCE)-MRI provides a promising alternative for noninvasive longitudinal assessment of the opening of the BBB. In DCE-MRI, the volume transfer coefficient K^{trans} is determined by fitting the dynamic contrast enhanced image intensities to mechanistic tracer kinetic models (Leach et al., 2005; Tofts, 2010). However, to date, K^{trans} MRI has only been used in a limited number of experimental TBI studies (Wei et al., 2011, 2012). One important reason is its low spatial and temporal resolution of the dynamic scans, and the poor image quality of the K^{trans} maps. To overcome this limitation, we recently developed a high-resolution K^{trans} MRI method for experimental TBI (Li et al.,

* Corresponding author at: Research Imaging Institute, University of Texas Health Science Center at San Antonio, 8403 Floyd Curl Dr, San Antonio, TX 78229, United States.
E-mail address: duongt@uthscsa.edu (T.Q. Duong).

http://dx.doi.org/10.1016/j.brainres.2016.05.036
0006-8993/

2014). This method uses a sensitive surface coil and optimized high temporal-resolution gradient-echo scans to achieve K^{trans} mapping with excellent SNR, high spatial resolution and reasonable spatial coverage. This method is compatible with the arterial spin labeling (ASL) method, which uses a separate neck coil to measure cerebral blood flow (CBF) (Duong, 2007; Shen et al., 2004a, 2004b) and other conventional T_2 and diffusion MRI methods.

In this study, we used the improved K^{trans} mapping approach to longitudinally evaluate the spatiotemporal evolution of BBB permeability from 1 h to 7 days post TBI using a controlled cortical impact (CCI) model. K^{trans} was compared with CBF disturbance, edema formation, and diffusion abnormalities. Comparison was also made with Evan's blue extravasation at selected time points.

2. Results

2.1. Sham animal results

Fig. 1 shows the K^{trans} map of the two sham rats and two representative TBI rats at day 2. T_2 maps from a sham and TBI animals are included to clarify the anatomical location of the K^{trans} maps. For the sham animals, there were no significant changes in CBF, T_2, ADC, and FA at all time points studied (data not shown), except there was some hyperintensity on the superficial cortical surface on the K^{trans} map (blue arrows) that is likely related to the craniotomy performed to induce the TBI. In comparison, the TBI brain shows much larger changes in the K^{trans} near the superficial cortical regions (green arrows).

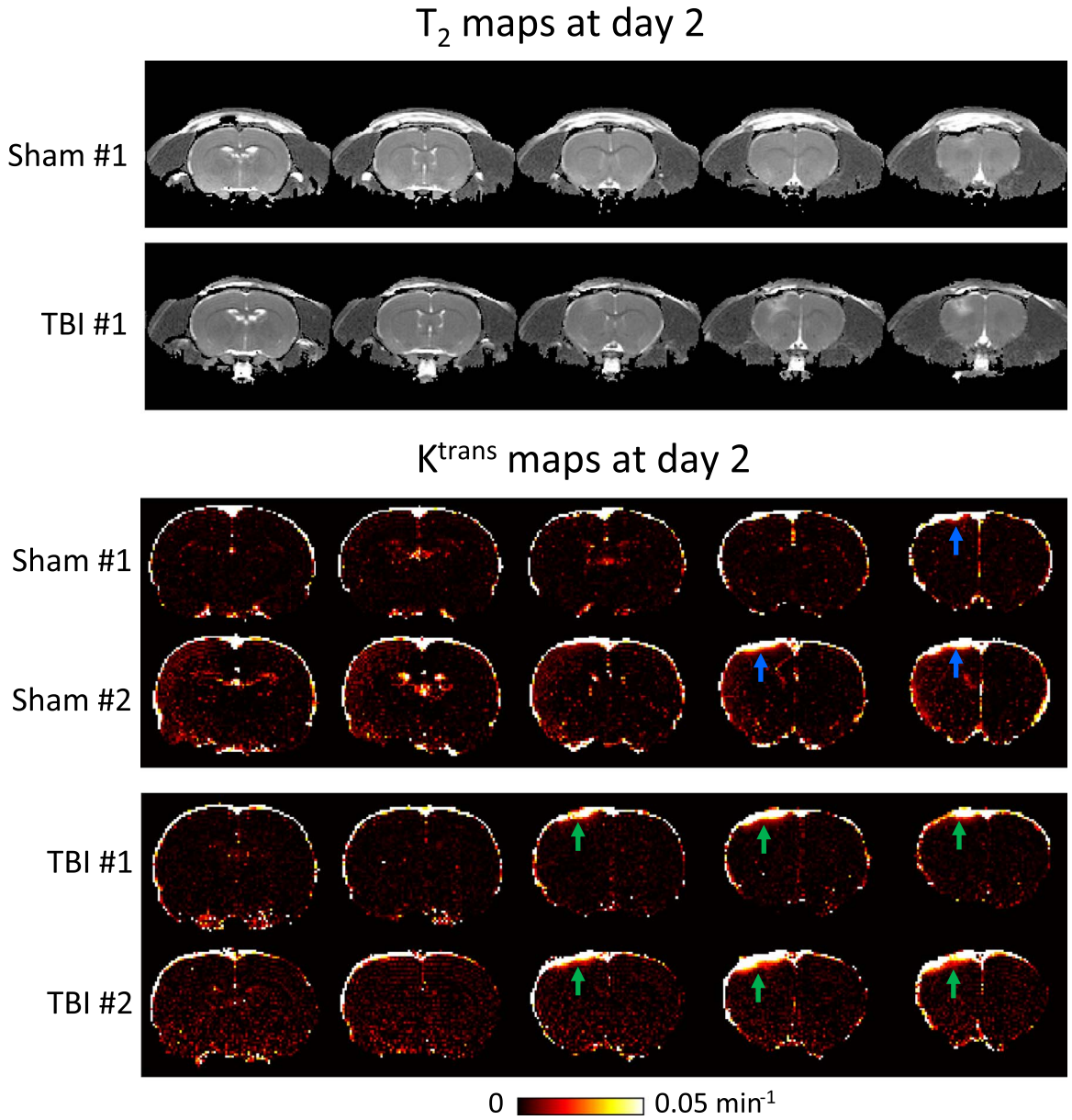

Fig. 1. The T_2 maps are shown to demonstrate the anatomical location of the K^{trans} maps and demonstrate the extent of the lesion on day 2 post-TBI (shown as hyperintensity within the map). The K^{trans} maps of sham and TBI animals at day 2. Blue arrow pointed to the increased K^{trans} on the superficial cortical surface of the sham animals that is related to the craniotomy. Green arrows pointed to much larger changes in the K^{trans} near the superficial cortical regions of the TBI animals.

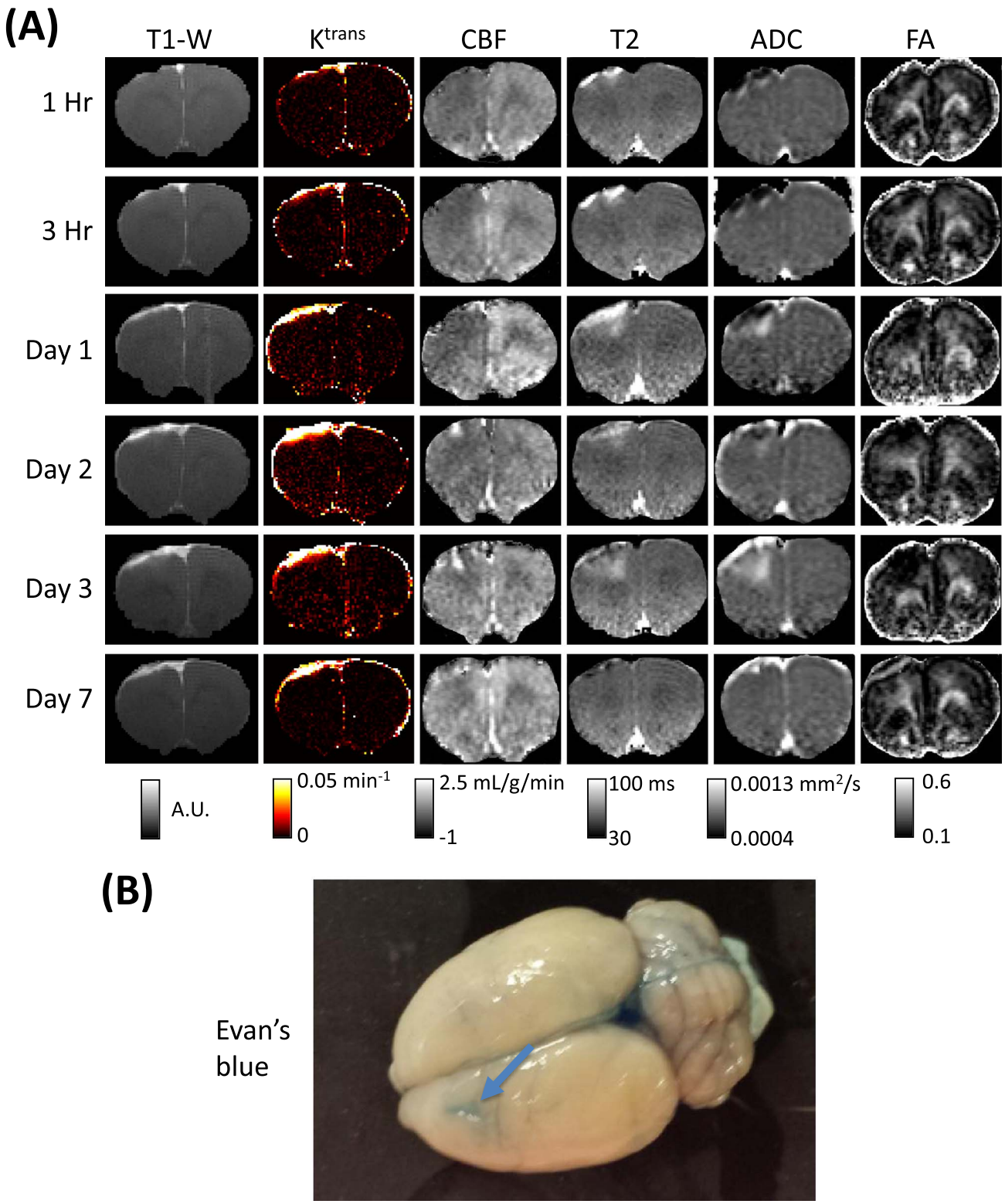

Fig. 2. (A) The representative maps of K^{trans}, CBF, T2, ADC and FA at different time points. Color Scale Bar for K^{trans}: 0–0.05 min^{-1}; Gray-scale Bar for CBF: 0–2.5 mL/gram/min, T_2: 30–100 ms, ADC: 0.0004–0.0013 mm^2/s, FA: 0.1–0.6. (B) Evan blue stains at 7 days from the same animal.

2.2. MRI contrast changes in a representative TBI rat

Fig. 2 shows representative single slices from T1-weighted (T1W) images, K^{trans}, CBF, T_2, ADC, and FA images from a single animal at 1 and 3 h, 1, 2, 3, and 7 days post-TBI. In the contralesional hemisphere, there were no significant changes in CBF, T_2, ADC, and FA at all time points studied, except for some hyperintensity on the superficial cortical surface on the T1W and K^{trans} map. It is noted that T1W images were calculated by averaging the same images used for calculating K^{trans}, and they revealed exactly the same patterns of BBB leakage, the difference is that T1W is qualitative while K^{trans} measures the quantitative flux across the BBB. Fig. 3 shows Evan's blue extravasation images of the brain sections from the same animals at the same time point.

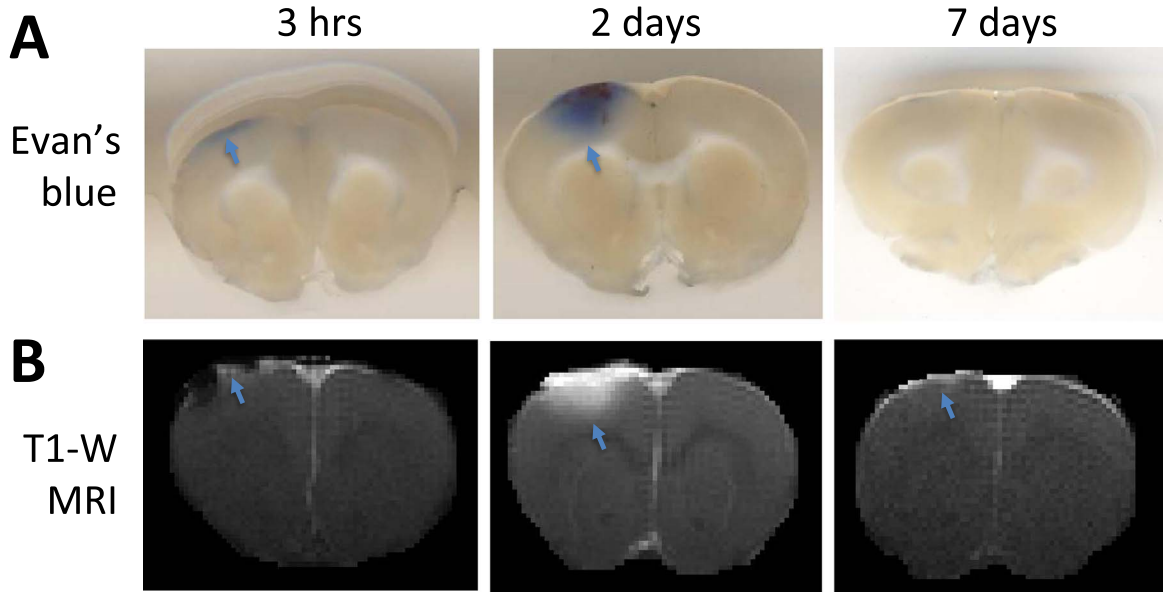

Fig. 3. Comparison of BBB leakage evaluated by Evan's Blue staining and T1 weighted MRI. (A) Evan's Blue staining at 3 h, 2 days and 7 days. (B) Corresponding T1-weighted MRI at the same spatial location and the same time point. Note: T1-weighted MRI was obtained by averaging dynamic scan for K^{trans}-MRI.

For these animals, the K^{trans} were not available due to the severe motion during the injection of contrast agent. However, the comparison between T1W and Evan's blue staining did identify the same brain regions with BBB leakage.

In the ipsilateral hemisphere, K^{trans} map showed hyperintensity, most prominently on the cortical surface of the impacted area (bright yellow and white pixels), indicative of disrupted BBB integrity. Abnormal K^{trans} was apparent at 1 h, and peaked on day 2–3 post-TBI and returning toward (but did not reach) normal on day 7.

CBF MRI showed perfusion deficits in and around the impact area at 1 and 3 h. Within the area of impact, hyperperfusion became evident by day 2 followed by mild hypoperfusion on day 7. The area of CBF deficit was larger than the K^{trans}, T_2, ADC, or FA abnormality at these time points.

T_2 MRI showed hyperintensity at the cortical surface just below the impacted area at 1 h. The T_2 map showed heterogeneous contrast across time points. The hyperintensity likely indicates vasogenic edema and hypointensity indicates possible hemorrhage.

ADC maps showed heterogeneous contrast under the impact area at 1 and 3 h and 1 and 2 days post TBI. The hyperintensity indicated on the ADC map likely represents vasogenic edema and hypointensity indicates possible cellular or cytotoxic edema. In the S1FL ipsilesional S1FL cortex, ADC was significantly elevated in the superficial layers by day 1, began to spread to deeper layers by day 1, peaked on day 3, and returned toward (but did not reach) normal values on day 7.

Abnormal FA was apparent within 1 h of the impact indicated by the black areas below the impacted areas (S1FL cortex). In the S1FL ipsilesional cortex, FA was significantly reduced at 1 and 3 h, remained reduced on days 1, 2 and 3 but returned toward normal values on day 7.

2.3. Spatial profiles of K^{trans}, CBF, T_2, ADC, and FA

To delineate the spatial profiles, the K^{trans}, CBF, T_2, ADC, and FA values were plotted as a function of the depth at 1 and 3 h, and 1, 2, 3 and 7 days post TBI (Fig. 4). K^{trans} maps were acquired using a FLASH sequence with short echo time and thus susceptibility artifacts were negligible. The ipsilesional K^{trans} changes were localized to the superficial layers from the surface to approximately 1 mm in depth, while much deeper (up to 2.5 mm) changes were found in CBF, T_2, ADC, and FA. There were significant differences between ipsilesional and contralesional data points displayed as closed circle ($p < 0.05$) at the corresponding time points.

In the contralesional hemisphere, K^{trans} had significant values at the exact brain surface (as expected due to the presence of intravascular contrast agent) and in layer B, but were not significant from zero at all other locations. The values of CBF, T_2, ADC, and FA for each ROI were not significantly different from one another over time ($P > 0.05$). There was however some fluctuation in the values based on the depth of the ROI for T_2 and FA, likely related to the brains' anatomy. The values for the contralesional hemisphere were averaged and plotted as a black dashed line on the ipsilesional graphs for comparison.

2.4. Temporal characteristics of K^{trans}, CBF, T_2, ADC, and FA

To evaluate the temporal characteristics, we excluded the surface layer, and grouped the data into 4 larger ROIs with each ROI having a thickness of 0.3 mm. The difference between ipsilesional and contralesional regions were calculated (Fig. 5). The ΔK^{trans} for the ROI at the superficial layer (0.2–0.8 mm, layer A) was significantly different at 1 h, 3 h and day 1 ($P < 0.05$), and continued to increase peaking on day 3 ($P < 0.05$) and then subsequently decreased toward normal at day 7 but remained significantly different ($P < 0.05$). The ΔK^{trans} for the ROI immediately underneath it (0.8–1.4 mm, layer B) showed no difference at 1 h, 3 h and day 1 ($P > 0.05$), significantly difference on day 3 ($P < 0.05$), and ended with no difference in K^{trans} on day 7 ($P > 0.05$). The ΔK^{trans} of two subsequent layers (1.4–2.0, layer C, and 2.0–2.6 mm, layer D) showed no difference at all the time points ($P > 0.05$).

CBF values showed perfusion deficits in and around the impact area from essentially the entire cortical depth (0.2–2.6 mm) during the acute phase (1 and 3 h). However, within the area of impact we detected an area of hyperperfusion that became evident on days 2 and 3. The CBF values returned towards contralesional values by day 7, with some layers (from 1.4 to 2.6 mm) to be slightly hypoperfused when compared to the homologous contralesional area.

T_2 values at 1 h after TBI increased reflecting hyperintensity just below the impacted area between 0.2 and 0.8 mm from the

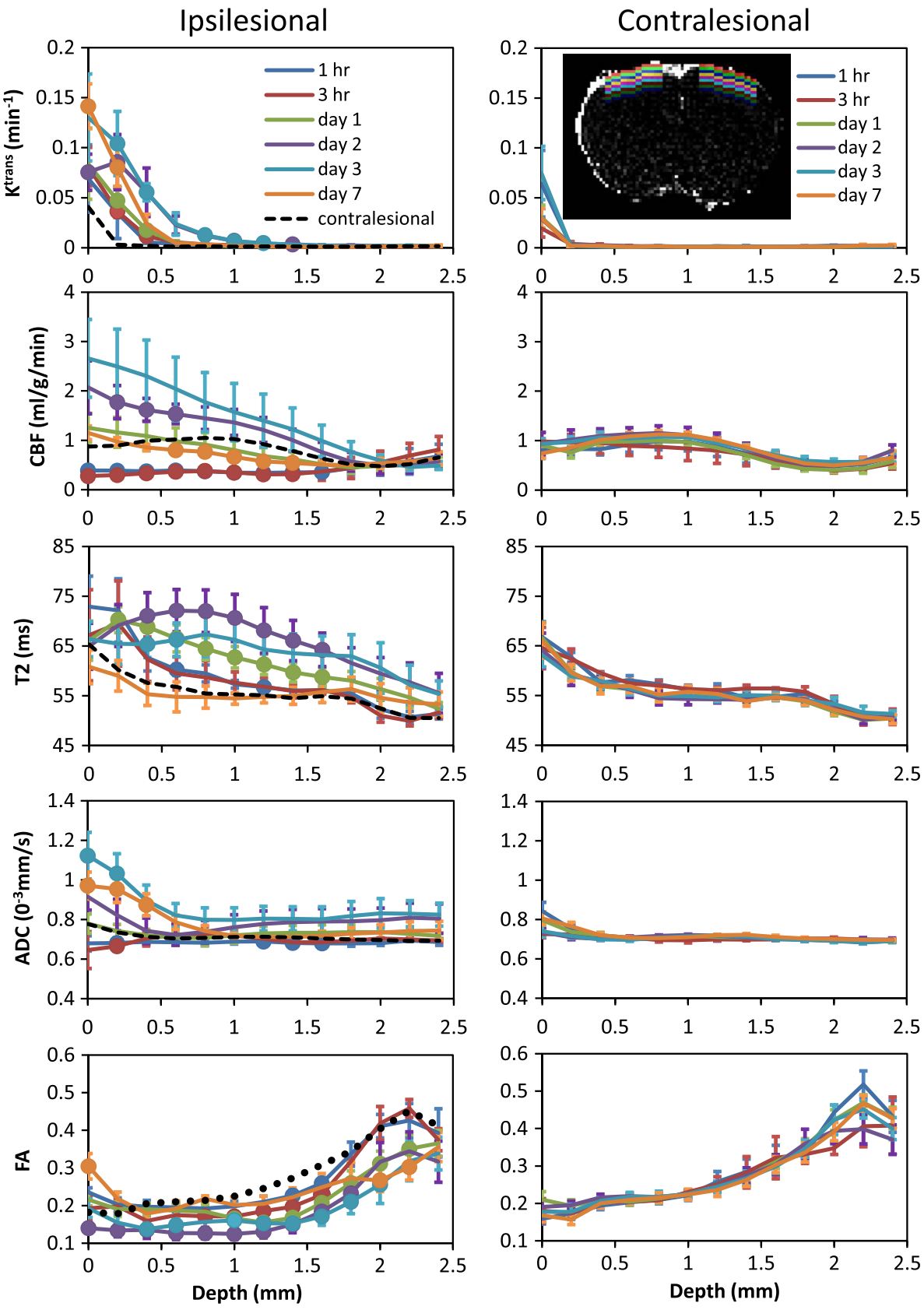

Fig. 4. Spatial profiles from cortical surface to corpus callosum of K^{trans}, CBF, T_2, ADC and FA. Data as represented as mean ± SEM. n=5, 4, 7, 6, 5 and 7, for 1 h, 3 h, 1, 2 and 7 days, respectively. Data points displayed as closed circle indicates significant different ($p < 0.05$) between the ipsilesional and contralesional cortex at the corresponding time points.

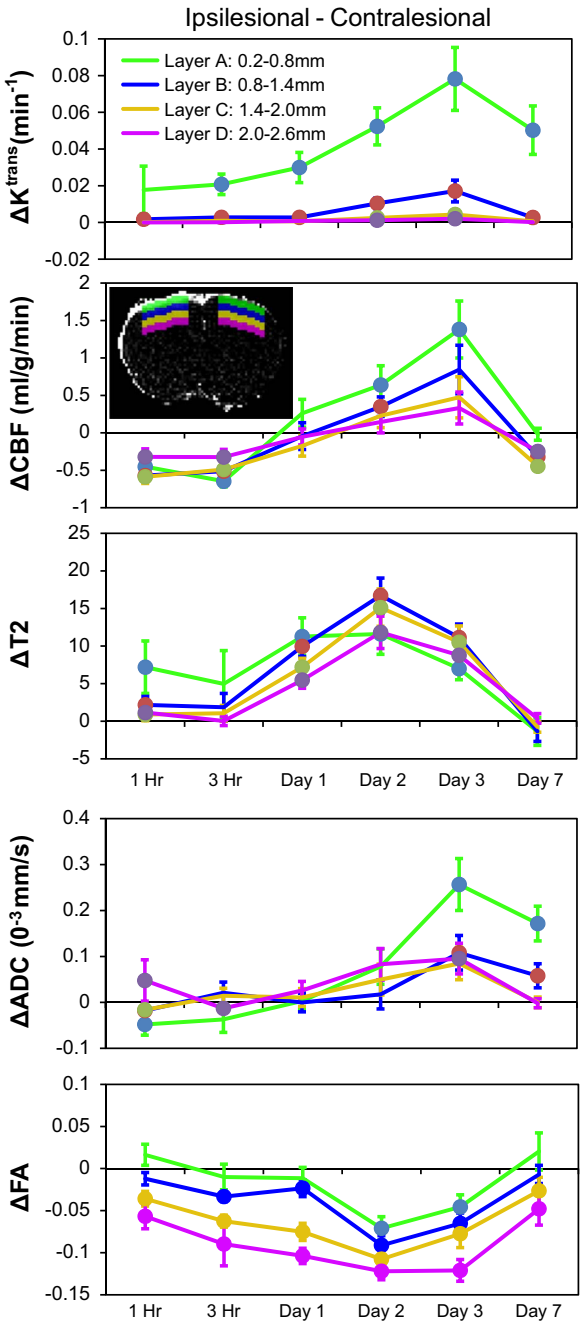

Fig. 5. Temporal profiles of K^{trans}, CBF, T_2, ADC and FA. Data as represented as mean ± SEM. n = 5, 4, 7, 6, 5 and 7, for 1 h, 3 h, 1, 2 and 7 days, respectively. Inset: ROIs of Layer A–D labeled in red, green, blue and yellow colors. Error bars are SEM.

cortical surface. The T_2 values peaked on day 2 for all layers analyzed, indicating a progression of edema formation. By day 7 the values at all depths were similar to those of the homologous contralesional areas.

The ADC immediately below the impacted area (0.2–0.8 mm) was lowered at 1 and 2 h, increased thereafter and peaked on day 3. The hyperintensity indicated by the ADC values likely represents vasogenic edema, and hypointensity indicates possible cellular or cytotoxic edema. At progressively deeper depths, ADC was slightly elevated.

FA values indicated decreased FA compared to the contralesional cortex between depths of 0.5–1.5 for all time points (Fig. 3). The FA values increased with increasing the depth similar to the contralesional hemisphere but remained lower between 2 and 2.5 mm for days 1, 2, and 7 (Fig. 4).

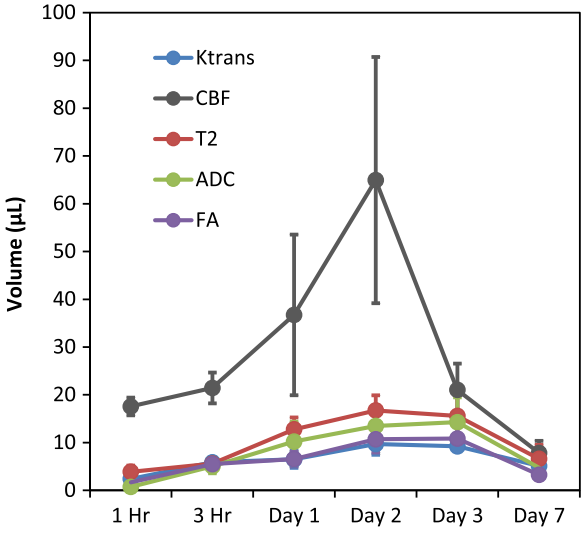

Fig. 6. Apparent lesions volumes determined by different (K^{trans}, CBF, T_2, ADC and FA) MRI contrasts. Error bars are SEM. Marker with closed circle means $p < 0.05$ between lesions volumes and the null hypothesis (no lesion).

2.5. Affected brain volumes

Fig. 6 depicts the group-averaged temporal progression of apparent abnormal volumes defined by K^{trans}, CBF, T_2, ADC, and FA abnormality following TBI. T_2 defined affected brain volumes were present at 3 h, consistently peaked on day 2, and were markedly reduced by day 7. The same trends were seen for K^{trans}, ADC, and FA, peaking on day 2 and returning towards normal values by day 7. CBF had the most dramatic changes in terms of abnormal brain volume.

3. Discussion

We evaluated the spatiotemporal evolution of K^{trans}, and compared it with cerebral blood flow (CBF) disturbance, T_2 edema formation, and diffusion abnormalities. Abnormal K^{trans} was most severe in superficial cortical layers around the impact site. This was in contrast to the widespread changes detected in CBF, T_2 and diffusion in both superficial cortical layers and deeper regions. Temporally, these contrasts also showed different initial alterations at 1 and 3 h, different time to peak contrast changes, and different recovery at 7 days.

3.1. Spatial distributions of K^{trans} and CBF, T_2, ADC and FA abnormalities

Our CBF, T_2, ADC and FA findings were consistent with our previous multi-parametric MRI of TBI (Long et al., 2014a). K^{trans} however exhibited significant differences from all of these contrasts. From the results, K^{trans} seems to be uncorrelated to the perfusion, edema, and diffusion changes, and its distribution is only determined by distance from the surface of the cerebral cortex. It is likely that this pattern results from the complex mechanical properties of the brain tissue. Mechanically, the brain is a nonlinear stain-rate sensitive viscoelastic material (Bilston, 2011). The effect of the mechanical impact on the brain has been extensively studied using finite element analysis methods (Chen and Ostoja-Starzewski, 2010; Takhounts et al., 2008; Ueno et al., 1995). Due to the nature of the open-skull cortical impact model used

within this study it is likely that using such methods, the simulated displacement, Von Mises stress, and sheer strain intensity profiles showed similar localized patterns to that of K^{trans} (Ueno et al., 1995). It is possible that BBB integrity is determined by one or a few components of these biomechanical properties that are predominately located to the superficial layers of the cerebral cortex, while the other contrasts are more sensitive to other components that are more diffuse.

Presumably BBB leakage should be related with brain tissue vasogenic edema, which could be detected as enhanced T_2 and ADC. Both T_2 and ADC demonstrated similar patterns of signal enhancement. This agreement further shows vasogenic edema. The more widespread CBF changes demonstrate a possible hemodynamic disturbance after TBI. However, K^{trans} only demonstrates hyperintensity in the area underneath the impact. This suggests that K^{trans} offers different and possibly complementary information.

3.2. Temporal evolutions of K^{trans}, CBF, T_2, ADC and FA

A previous study of BBB leakage in TBI using Evans Blue (EB) staining observed a biphasic pattern, with the first peak at 4 h and a second peak at 3 days (Başkaya et al., 1997). However, such a biphasic pattern is not observed in the current study. Instead, BBB leakage increased progressively from 1 h to 3 days, peaked at day 3 and then decreased towards normal by 7 days. Our results agree with the K^{trans} MRI of a weight drop-induced TBI in rabbit that showed increased K^{trans} 3 h post-TBI, that peaked at 3 days, and remained higher than sham-operated animals at day 7, while the perifocal lesion area showed increased K^{trans} at 1, 3 and 7 days (Wei et al., 2012). One possible reason for the discrepancy between K^{trans} MRI and EB staining is that K^{trans} MRI and EB staining measure different aspects of BBB leakage. K^{trans} MRI indirectly measures the leakage of a small-molecular-weight gadodiamide (592 Da), whereas the EB method measures the leakage of EB bound to serum proteins (65 kDa) that is two-orders of magnitude larger in size. This suggests that the MRI based method has increased sensitivity to smaller disruptions in the BBB compared to the EB based method.

3.3. Significance of BBB leakage on tissue fate

While K^{trans}, CBF, T_2 and diffusion have dramatically different spatial and temporal evolutions, their impact on tissue fate can be very different. Tissue fate is directly linked to the mechanical stresses associated with TBI that cause damage to blood vessels that can produce cortical hemorrhages, contusions and hematomas that may result in ischemic tissue. Additionally, the mechanical forces also cause axonal and tissue stretching that further increases structural damage to blood vessels and cells within the impacted area. A previous TBI study using the same CCI model observed that obvious tissue cavitation (or tissue loss) were also localized to the superficial cortical regions that were close to the impact site (Long et al., 2014a). This pattern of gross tissue loss agrees well with the patterns of K^{trans}, but is not consistent with the lesion volumes determined by CBF, T_2 and diffusion MRI methods. This result suggests that K^{trans} may provide a more relevant quantitative marker to predict the tissue fate. The critical role of BBB leakage is further supported by successful reduction of TBI damage through stabilization of the BBB (Thal and Neuhaus, 2014). In addition to tissue cavitation and gross tissue loss, Nissl staining revealed abnormally appearing cells that are spread between healthy neuronal cells in regions that surround the impact site (Long et al., 2014a). The impact of BBB leakage, edema and cerebral blood flow on cell fate in these bordering regions requires further investigation.

3.4. Comparison with Evan's blue

A major key finding of this study is that the brain regions with BBB leakage identified by Evan's blue extravasation agrees with regions determined by K^{trans} maps reasonably well in the same animals at various time points after TBI. It is important that the BBB leakage revealed by Evan's blue was also localized to the superficial cortical layers in this mild TBI model. This is consistent with a previous study from our laboratory (Li et al., 2014). Although the sample size was small, we noted that Evan's blue leakage appeared to change across time points and across animals. It could be challenging for Evan's blue method to detect multiphasic BBB leakage (if present) with small sample sizes. K^{trans} MRI thus has the potential to offer a unique means to longitudinally monitor BBB changes in TBI, which could have clinical utility in injury staging and treatment targeting.

3.5. Limitations

(i) Different MRI modalities used herein gave rise to varying degrees of susceptibility artifacts, which confound comparisons amongst different modalities. For example, diffusion MRI used echo-planar imaging which has some surface susceptibility artifacts, whereas K^{trans} MRI used FLASH sequence with short echo time which has negligible susceptibility artifacts. Comparison across modalities needs to be made with caution. (ii) A drawback of this study is that we did not perform quantitative group comparison between Evan's blue and MRI data because of the small sample sizes and differences in methodologies that measures somewhat different aspects of BBB integrity, amongst others. Some of the differences in methodologies include difference in size and properties of the tracers, the duration over which the leakage measurements are made, etc. Future studies will need to be carefully designed to enable quantitative comparison in the same animals. (iii) K^{trans} MRI method requires an administration of an exogenous contrast agent, which limits repeated measurements. Diffusion-weighted perfusion MRI which measures vascular water exchange can be explored without a contrast agent can be explored (St. Lawrence et al., 2012).

4. Conclusion

In a CCI model of TBI, the K^{trans} increase was primarily localized to the superficial cortical layers that were adjacent to the impact site, which were different from the much deeper and widespread changes of CBF disturbance, edema formation, and diffusion abnormalities. Temporally, the K^{trans} increase was present at 1 h, increased progressively over time, peaked at day 3 and then recovered towards normal at 7 days. These results suggest that BBB disruption, edema formation, blood flow disturbance and diffusion changes are related to different components of the mechanical impact, and may play different roles in determining injury progression and tissue fate processes in TBI.

5. Experimental procedures

5.1. Controlled cortical impact (CCI) model of rat TBI

All animal procedures were approved by the Institutional Animal Care and Use Committee of the University of Texas Health Science Center at San Antonio. The TBI model was performed as previously described (Long et al., 2014b; Talley Watts et al., 2014). Briefly, male Sprague Dawley rats (250–350 g, n=10 TBI, and 2 sham) were anesthetized initially with 5% isoflurane mixed with

room air and subsequently maintained at 1.2% isoflurane throughout all surgical and imaging procedures. The animal was secured in a stereotaxic frame and a surgical incision was made posterior from the impact site (at the level of the cerebellum) to prevent artifacts during MRI acquisition and the periosteum was removed over the impact site. A Ø5 mm craniotomy was created over the left forelimb primary somatosensory cortex (S1FL: +0.25 mm anterior and 3.5 mm lateral to bregma), exposing the dura matter. The intact dura matter was impacted using a pneumatic controlled cortical impactor (Precision Systems and Instrumentation, LLC, Fairfax Station, Virginia) fitted with a Ø3 mm tip (5.0 m/s, 250 μs dwell time, 1 mm depth) to mimic a mild focal TBI. Following the impact the cranial opening was sealed with bone wax, the scalp sutured closed and antibiotic ointment applied. Saline was injected under the skin to facilitate the removal of air pockets between the scalp and the skull to minimize artifacts during MRI acquisition. For the sham group, the depth parameter of the CCI sequence was adjusted such that there was no physical impact on the tissue. Buprenex (0.05 mg/kg) was given subcutaneously every 12 h for three days for pain.

At selected time points, animals were sacrificed for Evan's blue extravasation. Evans Blue (EB) extravasation was evaluated in 8 out of 10 animals at various time points (2 at 3 h, 3 at 2 days, and 3 at 7 days). As a result, the number of animals for MRI data ranged from 4 to 7 for each time point.

5.2. Brain MRI

MRI was acquired on the day of the TBI procedure, at 1 and 3 h post TBI and on days 1, 2, 3, and 7 following TBI onset on a Bruker 7T BioSpec MRI scanner. A custom-made surface transceiver coil was used for brain imaging. The animal was secured in a custom built, MRI compatible, rat head stereotaxic holder with ear and tooth bars, and was scanned under 1.2% isoflurane. End-tidal CO_2 was monitored via a SurgiVet capnometer (Smith Medical, Waukesha, WI, USA). Noninvasive end-tidal CO_2 values have been calibrated previously against invasive blood gas samplings under identical settings. The heart rate and blood-oxygen saturation levels were also monitored and maintained at physiological levels using a MouseOx system (STARR Life Science, Oakmont, PA, USA).

K^{trans}-MRI (19.4 min): All K^{trans} MRI data were acquired using a 2D multi-slice FLASH sequence. A pre-scan was used to determine the flip angle and M_0 distribution, which included 3 FLASH scans with different TRs: 64 ms (scan 1), 200 ms (scan 2) and 3000 ms (scan 3). The rest of imaging parameters were the same: five 1.0-mm coronal images, TE = 2 ms, FOV = 2.56 × 2.56 cm^2, 128 × 128 data matrix and 30° nominal flip angle. The pre-scan took 7.4 min Dynamic scans use a TR of 64 ms, and otherwise identical sequence parameters. After baseline data were acquired for 2 min, a bolus (0.2 mL/kg) of gadodiamide (Omniscan™, GE Healthcare, USA) was injected intravenously through the tail vein, during which the dynamic scan was continued. A total of 90 dynamic images were acquired with a temporal resolution of 8 s, lasting 12 min in total.

CBF (6 min): CBF images were attained using the continuous arterial spin labeling technique with single-shot, gradient-echo, echo-planar imaging (EPI) sequence with partial Flourier (5/8) acquisition (Shen et al., 2003, 2004a, 2005). Continuous arterial spin labeling employed a 2.7 s square radiofrequency pulse to the labeling coil. The other parameters were: seven 1.0-mm coronal images, FOV = 2.56 × 2.56 cm, matrix 96 × 96 and reconstructed to 128 × 128, FOV = 2.56 × 2.56 cm, TR = 3 s (90° flip angle), TE = 10.2 ms, and 60 averages.

Diffusion MRI (3.5 min): DTIs were obtained with a b = 0 s/mm^2 in a single direction and a b = 1200 s/mm^2 with 30 directions. Echo-planar imaging scans (EPI) with partial Fourier (5/8) were also acquired using the following settings: seven 1.0-mm coronal images, FOV = 2.56 × 2.56 cm, matrix 96 × 96 and reconstructed to 128 × 128, single shot, TR = 3 s, TE = 32 ms, and 2 averages (Shen et al., 2003, 2004a, 2005).

T_2 mapping (9.5 min): T_2-weighted images were acquired using fast spin-echo (FSE) sequence with TR = 3 s (90° flip angle), effective TE = 18, 54, 90 and 126 ms, 4 echo train length. The other parameters were: seven 1.0-mm coronal images, FOV = 2.56 × 2.56 cm, matrix 96 × 96 and reconstructed to 128 × 128 and 8 averages (Shen et al., 2003, 2004a, 2005).

5.3. Image analysis

K^{trans} values were calculated as described previously (Li et al., 2014). Briefly, the flip angle and M_0 distribution were determined from the pre-scan, which were used to calculate the dynamic T_1 changes. The ΔT_1 was calculated by subtracting dynamic T_1 values from the baseline T_1. AIF was determined by scaling a group AIF determined by radiolabeled Gd-DTPA using the method by Ewing and colleagues (Nagaraja et al., 2008). K^{trans} was obtained by fitting ΔT_1 and AIF to the nested Kety model with model selection using F-statistic. CBF, T_2, ADC, and FA maps were calculated as previously described (Danker and Duong, 2007; Shen et al., 2003, 2005; Sicard et al., 2003; Sicard and Duong, 2005).

Both the K^{trans} mapping and the subsequent ROI-based analysis used an in-house developed Matlab-based program. For ROI analysis, the images of multiple contrasts were loaded into DCE-Tool. A line with a thickness of 1 voxel was drawn to cover the exact boundary of the brain tissue in both the ipsilesional and corresponding contralesional side. These two lines were subsequently shifted to derive multiple ROIs along the depth of the brain, as shown in Fig. 1. This ROI drawing process was repeated for each image contrast to accommodate the different characteristics in image distortions associated with each pulse sequence. The contrast values within the same ROI were averaged to tabulate the K^{trans}, CBF, T_2, ADC, and FA values across all time points. The volumes with significant contrast changes were manually defined using DCE-Tool.

5.4. Histology

BBB permeability was evaluated using Evans Blue (EB) extravasation as described previously (Gürsoy-Özdemir et al., 2000; Jiang et al., 2014). Briefly, 1 mL of 4% EB prepared in clinical grade saline (Sigma-Aldrich, USA) was injected into the tail vein immediately after the dynamic scan and allowed to circulate for 1 h. The rats were then transcardially perfused with heparinized saline solution followed by 4% paraformaldehyde. Brains were removed and cut into 1 mm slices to match the slice orientation and position of the MRI scans. The brain sections were imaged using an optical scanner. The brain regions stained with blue color indicate the leakage of EB bound to plasma albumin that moved across the impaired BBB. Corresponding K^{trans} and EB images were compared visually on the same animal. Quantitative group comparison with MRI data was not performed due to small sample size.

5.5. Statistical analysis

Paired *t*-tests were used to compare K^{trans}, CBF, T_2, ADC, and FA abnormality between the ipsi- and contra-lesional sides. A one-way ANOVA was also performed on each ROI analyzed to determine if there was statistical significance between time points. Fluctuations between time points of lesion volumes were compared with paired *t*-tests. A one-way ANOVA was used to examine statistical significance between time points. Values are presented as mean ± standard error of the mean with $p < 0.05$ indicates statistical significance.

Acknowledgment

This research was funded in part by NIH/NINDS R01 NS45879 (TQD), a TL1 grant (JAL) and KL2 TR001118 (LTW) via the Clinical Translational Science Awards (CTSA, parent grant 8UL1TR000149 and TL1TR001119). This study was supported in part by UL1 TR001119 via the Clinical Translational Science Awards (WL), and a research grant from William & Ella Owens Medical Research Foundation (WL), and a Scientist Development Grant 15SDG26020003 from American Heart Association (WL).

References

Adelson, P.D., Whalen, M., Kochanek, P., Robichaud, P., Carlos, T., 1998. Blood brain barrier permeability and acute inflammation in two models of traumatic brain injury in the immature rat: a preliminary report. Acta Neurochir. 71, 104–106.

Başkaya, M.K., Muralikrishna Rao, A., Doğan, A., Donaldson, D., Dempsey, R.J., 1997. The biphasic opening of the blood–brain barrier in the cortex and hippocampus after traumatic brain injury in rats. Neurosci. Lett. 226, 33–36.

Bilston, L.E., 2011. Neural Tissue Biomechanics. 3. Springer Science & Business Media, Berlin, Heidelberg.

Chen, Y., Ostoja-Starzewski, M., 2010. MRI-based finite element modeling of head trauma: spherically focusing shear waves. Acta Mech. 213, 155–167.

Chodobski, A., Zink, B.J., Szmydynger-Chodosbska, J., 2011. Blood-brain barrier pathophysiology in traumatic brain injury. Transl. Stroke Res. 2 (4), 492–516.

Danker, J.F., Duong, T.Q., 2007. Quantitative regional cerebral blood flow MRI of animal model of attention-deficit/hyperactivity disorder. Brain Res. 1150, 217–224.

Dempsey, R.J., Baskaya, M.K., Dogan, A., 2000. Attenuation of brain edema, blood-brain barrier breakdown, and injury volume by ifenprodil, a polyamine-site N-methyl-D-aspartate receptor antagonist, after experimental traumatic brain injury in rats. Neurosurgery 47, 399–406.

Duong, T.Q., 2007. Cerebral blood flow and BOLD fMRI responses to hypoxia in awake and anesthetized rats. Brain Res. 1135, 186–194.

Gürsoy-Özdemir, Y., Bolay, H., Saribaş, O., Dalkara, T., 2000. Role of endothelial nitric oxide generation and peroxynitrite formation in reperfusion injury after focal cerebral ischemia. Stroke 31, 1974–1981.

Jiang, Z., Chen, C.-H., Chen, Y.-Y., Han, J.-Y., Riley, J., Zhou, C.-M., 2014. Autophagic effect of programmed cell death 5 (PDCD5) after focal cerebral ischemic reperfusion injury in rats. Neurosci. Lett. 566, 298–303.

Leach, M.O., Brindle, K., Evelhoch, J., Griffiths, J.R., Horsman, M.R., Jackson, A., Jayson, G.C., Judson, I.R., Knopp, M., Maxwell, R.J., 2005. The assessment of anti-angiogenic and antivascular therapies in early-stage clinical trials using magnetic resonance imaging: issues and recommendations. Br. J. Cancer 92, 1599–1610.

Li, W., Long, J.A., Watts, L.T., Jiang, Z., Shen, Q., Li, Y., Duong, T.Q., 2014. A quantitative MRI method for imaging blood-brain barrier leakage in experimental traumatic brain injury. PLoS One 9, e114173.

Long, J.A., Watts, L.T., Chemello, J., Huang, S., Shen, Q., Duong, T.Q., 2014a. Multiparametric and longitudinal MRI characterization of mild Traumatic Brain Injury in rats. J. Neurotrauma 32, 598–607.

Long, J.A., Watts, L.T., Chemello, J., Huang, S., Shen, Q., Duong, T.Q., 2014b. Multiparametric and longitudinal MRI characterization of mild traumatic brain injury in rats. J. Neurotrauma.

Nagaraja, T.N., Karki, K., Ewing, J.R., Croxen, R.L., Knight, R.A., 2008. Identification of variations in blood-brain barrier opening after cerebral ischemia by dual contrast-enhanced magnetic resonance imaging and T1sat measurements. Stroke 39, 427–432.

Shen, Q., Fisher, M., Sotak, C.H., Duong, T.Q., 2004a. Effects of reperfusion on ADC and CBF pixel-by-pixel dynamics in stroke: characterizing tissue fates using quantitative diffusion and perfusion imaging. J. Cereb. Blood Flow Metab. 24, 280–290.

Shen, Q., Meng, X., Fisher, M., Sotak, C.H., Duong, T.Q., 2003. Pixel-by-pixel spatiotemporal progression of focal ischemia derived using quantitative perfusion and diffusion imaging. J Cereb. Blood Flow Metab. 23, 1479–1488.

Shen, Q., Ren, H., Fisher, M., Bouley, J., Duong, T.Q., 2004b. Dynamic tracking of acute ischemic tissue fates using improved unsupervised ISODATA analysis of high-resolution quantitative perfusion and diffusion data. J Cereb. Blood Flow Metab. 24, 887–897.

Shen, Q., Ren, H., Cheng, H., Fisher, M., Duong, T.Q., 2005. Functional, perfusion and diffusion MRI of acute focal ischemic brain injury. J Cereb. Blood Flow Metab. 25, 1265–1279.

Shlosberg, D., Benifla, M., Kaufer, D., Friedman, A., 2010. Blood–brain barrier breakdown as a therapeutic target in traumatic brain injury. Nat. Rev. Neurol. 6 (7), 393–403.

Sicard, K., Shen, Q., Brevard, M.E., Sullivan, R., Ferris, C.F., King, J.A., Duong, T.Q., 2003. Regional cerebral blood flow and BOLD responses in conscious and anesthetized rats under basal and hypercapnic conditions: implications for functional MRI studies. J. Cereb. Blood Flow Metab. 23, 472–481.

Sicard, K.M., Duong, T.Q., 2005. Effects of hypoxia, hyperoxia and hypercapnia on baseline and stimulus-evoked BOLD, CBF and CMRO2 in spontaneously breathing animals. NeuroImage 25, 850–858.

St. Lawrence, K.S., Owen, D., Wang, D.J.J., 2012. A two-stage approach for measuring vascular water exchange and arterial transit time by diffusion-weighted perfusion MRI. Magn. Reson. Med. 67, 1275–1284.

Takhounts, E.G., Ridella, S.A., Hasija, V., Tannous, R.E., Campbell, J.Q., Malone, D., Danelson, K., Stitzel, J., Rowson, S., Duma, S., 2008. Investigation of traumatic brain injuries using the next generation of simulated injury monitor (SIMon) finite element head model. Stapp Car Crash J. 52, 1–31.

Talley Watts, L., Long, J.A., Chemello, J., Van Koughnet, S., Fernandez, A., Huang, S., Shen, Q., Duong, T.Q., 2014. Methylene blue is neuroprotective against mild traumatic brain injury. J. Neurotrauma 31, 1063–1071.

Thal, S.C., Neuhaus, W., 2014. The blood–brain barrier as a target in traumatic brain injury treatment. Arch. Med. Res. 45, 698–710.

Tofts, P.S., 2010. T1-weighted DCE imaging concepts: modelling, acquisition and analysis. Signal 500, 400.

Ueno, K., Melvin, J.W., Li, L., Lighthall, J.W., 1995. Development of tissue level brain injury criteria by finite element analysis. J. Neurotrauma 12, 695–706.

Wei, X.-E., Zhang, Y.-Z., Li, Y.-H., Li, M.-H., Li, W.-B., 2012. Dynamics of rabbit brain edema in focal lesion and perilesion area after traumatic brain injury: a MRI study. J. Neurotrauma 29, 2413–2420.

Wei, X.-E., Wang, D., Li, M.-H., Zhang, Y.-Z., Li, Y.-H., Li, W.-B., 2011. A Useful tool for the initial assessment of blood–brain barrier permeability after traumatic brain injury in rabbits: dynamic contrast-enhanced magnetic resonance imaging. J. Trauma Acute Care Surg. 71, 1645–1651.